JOURNAL OF GEOMETRIC MECHANICS
©American Institute of Mathematical Sciences
Volume **4**, Number **2**, June **2012**
doi:10.3934/jgm.2012.4.xx
pp. **X–XX**

VARIATIONAL INTEGRATORS FOR HAMILTONIZABLE NONHOLONOMIC SYSTEMS

Oscar E. Fernandez

Department of Mathematics
Wellesley College
Wellesley, MA 02482, USA

Anthony M. Bloch

Department of Mathematics
University of Michigan
Ann Arbor, MI 48109, USA

Peter J. Olver

School of Mathematics
University of Minnesota
Minneapolis, MN 55455, USA

Abstract. We report on new applications of the Poincaré and Sundman time-transformations to the simulation of nonholonomic systems. These transformations are here applied to nonholonomic mechanical systems known to be Hamiltonizable (briefly, nonholonomic systems whose constrained mechanics are Hamiltonian after a suitable time reparameterization). We show how such an application permits the usage of variational integrators for these non-variational mechanical systems. Examples are given and numerical results are compared to the standard nonholonomic integrator results.

Introduction. It is well known that the dynamical equations of motion of unconstrained mechanical systems follow from a variational principle, namely Hamilton's principle of stationary action [1, 26]. In the 1970s and 1980s several researchers discretized this continuous variational principle and developed the discrete Euler-Lagrange equations (see [27] and references therein for a historical account). Like its continuous counterpart, this discrete variational mechanics preserves many of the constants of motion between timestep increments, such as the energy and momentum, as well as the symplectic form, under appropriate assumptions [21, 27]. The resulting numerical integrators, termed mechanical integrators, have found application in molecular dynamics simulations [34, 24, 23] and planetary motion [23], as well as in satellite dynamics [23]. For fixed timesteps, it was shown in [18] that a mechanical integrator for a non-integrable mechanical system with symmetry can at best preserve two of the three quantities mentioned above. For this reason, fixed timestep mechanical integrators are named according to what invariants they do preserve. In particular, mechanical integrators preserving the discretized symplectic form and momentum are known as *variational integrators*.

2000 *Mathematics Subject Classification.* Primary: 37J60; Secondary: 34K28.
Key words and phrases. Nonholonomic Systems, Hamiltonization, Variational Integrators.

Variational integrators for mechanical systems with position constraints (known as holonomic constraints) were developed shortly after the formulation of discrete variational mechanics (see [32] and Section 3.4 of [27] and references therein). However, for mechanical systems subject to non-integrable constraints on the velocities (known as nonholonomic systems), developing corresponding integrators remained a challenge for some time. The inherent difficulty arises from the fact that the equations of motion of a general nonholonomic system on a symplectic manifold (T^*Q, ω) (here ω is the symplectic form) follow not from Hamilton's principle, but instead from the Lagrange-d'Alembert principle [1]. The most immediate consequence is that the nonholonomic flow does not preserve the symplectic form ([8], Section 3.4.1). Thus, the basis of discrete variational mechanics (the discretization of Hamilton's principle) does not apply to nonholonomic systems. Despite this difficulty, the development of a "nonholonomic integrator" was achieved more recently in [9]. The authors discretized the Lagrange-d'Alembert principle to arrive at a mechanical integrator which preserves the evolution of the discretized symplectic form ω under the nonholonomic flow. In addition, for a nonholonomic system with symmetry, their nonholonomic integrator satisfies a discrete version of the nonholonomic momentum equation[1].

Historically, although the fact that nonholonomic mechanics is not variational (meaning the governing equations of motion do not follow from Hamilton's principle) was proved as early as 1899 by Korteweg [22], there have since been many attempts to "Hamiltonize" nonholonomic systems. In light of Korteweg's result, this is impossible to accomplish for the "full" nonholonomic system, which is generally a coupled set of first-order kinematic equations (in the simplest case of linear homogeneous nonholonomic constraints) and second-order dynamical equations. However, under certain symmetry conditions the kinematic equations decouple from the dynamics, in which case one can investigate the possibility of "Hamiltonizing" the second-order dynamical equations. The most successful early attempts to do so were made by the Russian mathematician S.A. Chaplygin in 1903, motivating the name *Chaplygin System* [1] (Section 5.4). In [6, 7] he showed that for nonholonomic systems in two degrees of freedom (q_1, q_2) which preserve a scaled symplectic form $f(q_1, q_2)\omega$ for some *multiplier* $f \in C^2(Q)$ one can define the time reparameterization $d\tau = f(q)\, dt$ such that the nonholonomic equations become the Euler-Lagrange equations of the time-reparameterized nonholonomic Lagrangian. This result is known as the *Chaplygin Reducing Multiplier Theorem*, and has been the subject of recent renewed interest (see [15] and references therein). It has recently been applied to nonholonomic Hamilton-Jacobi theory [31], and to the study of the integrability of rolling bodies (see [4] and references therein).

In this paper we apply Chaplygin's theorem to develop two new mechanical integrators for Chaplygin nonholonomic systems for which Chaplygin's theorem applies (termed Chaplygin Hamiltonizable). The mechanical integrators developed, in contrast to the nonholonomic integrator discussed above, are variational, that is, they are developed by discretizing Hamilton's principle. The examples developed in Section 5 suggest that, in general, the new algorithms accurately simulate the second-order dynamics of the Chaplygin Hamiltonizable system, and in some cases outperform the results obtained by the nonholonomic integrator. These results

[1]Unlike unconstrained mechanics, infinitesimal symmetries of nonholonomic systems do not necessarily lead to momentum conservation laws. Instead, the corresponding momentum maps evolve according to the nonholonomic momentum equation [1] (Section 5.5).

confirm earlier studies [29] showing that the combination of Hamiltonization and variational integrators can lead to superior numerical schemes for simulating the dynamics of many of the relevant nonholonomic systems.

The paper is organized as follows. We begin with a review of nonholonomic mechanics in Section 1, followed by a review of variational and nonholonomic integrators in Section 2. We discuss Chaplygin's theorem in more detail in Section 3 in preparation for the introduction of the new integrators in Section 4. In Section 4.1 we introduce the *Hamiltonized discrete Euler-Lagrange algorithm*, an integrator which proceeds in discretized τ-time. In Section 4.2 we introduce the *Poincaré transformed Hamiltonized discrete Euler-Lagrange algorithm*, which proceeds in t-time, and makes use of the so-called *Poincaré transformation* [23] (Chapter 9). Finally, we compare the performance of the two new integrators with that of the nonholonomic integrator for three examples in Section 5, and indicate possible applications and directions for future research in the Conclusion.

1. Nonholonomic Chaplygin systems.

Consider a mechanical system on an n-dimensional Riemannian configuration manifold Q with metric g and with regular Lagrangian $L\colon TQ \to \mathbb{R}$. We assume that $L = T - V$, where $T\colon TQ \to \mathbb{R}$ is the *kinetic energy* given by $T(q,\dot{q}) = \frac{1}{2} g_{ij}\dot{q}^i\dot{q}^j$, $i,j = 1,\dots,n$, where g_{ij} are the components of g, and $V : Q \to \mathbb{R}$ is the *potential energy* (we identify V with its lift to TQ). We note that we will adhere to the Einstein summation convention for repeated indices throughout.

Suppose that we now define a *constraint distribution* $\mathcal{D} \subset TQ$ by the one-forms $\{\omega^a\}_{a=1}^k$, $k < n$, as

$$\mathcal{D} = \{v \in TQ \,|\, \omega^a(v) = 0,\ a = 1,\dots,k\}. \tag{1}$$

We will assume that the constraints are linear and homogeneous, so that locally $\omega^a(v) = c^a_j(q)\dot{q}^j$, and that $\mathcal{D}$ has constant rank. Then the triple $(Q, L, \mathcal{D})$ is known as a *nonholonomic mechanical system* [1].

Now, suppose that a k-dimensional Lie group G acts on Q such that $M := Q/G$ is a manifold; this happens, for example, if G acts freely and properly on Q. Let $\mathfrak{g}$ be the Lie algebra of G, and ξ_Q the infinitesimal generator on Q corresponding to $\xi \in \mathfrak{g}$. We assume that its lifted action leaves L and $\mathcal{D}$ invariant, and that at each $q \in Q$, the tangent space T_qQ can be decomposed as

$$T_qQ = \mathfrak{g}_Q \oplus \mathcal{D}_q, \quad \text{where} \quad \mathfrak{g}_Q\big|_q = \{\xi_Q(q) \,|\, \xi \in \mathfrak{g}\} \tag{2}$$

is the tangent to the orbit through $q \in Q$ [1] (Section 2.8). Then we will call $(Q, L, \mathcal{D}, G)$ a *Chaplygin nonholonomic system* [1]. This setup gives rise to a principal bundle $\pi\colon Q \to M$, with principal connection $\mathcal{A}\colon TQ \to \mathfrak{g}$ such that $\ker \mathcal{A} = \mathcal{D}$. This connection can then be used to decompose any tangent vector $v_q \in T_qQ$ into horizontal and vertical parts:

$$v_q = \mathrm{hor}(v_q) + \mathrm{ver}(v_q), \tag{3}$$
$$\text{where} \qquad \mathrm{hor}(v_q) = v_q - (\mathcal{A}_q(v_q))_Q(q), \qquad \mathrm{ver}(v_q) = (\mathcal{A}_q(v_q))_Q(q).$$

We can now form the reduced velocity phase space TQ/G, and the Lagrangian L induces the reduced Lagrangian $l\colon TQ/G \to \mathbb{R}$ satisfying $L = l \circ \pi_{TQ}$, where $\pi_{TQ}\colon TQ \to TQ/G$ is the standard projection. Furthermore, the decomposition (3) gives rise to the *reduced constrained Lagrangian* $l_c\colon TM \to \mathbb{R}$ given by $l_c(r,\dot{r}) :=$

$L(q, \mathrm{hor}(\dot{q}))$, where $r = \pi(q)$ and $\dot{r} = T_q\pi(\dot{q})$. Locally, we will write the reduced constrained Lagrangian as

$$l_c(r, \dot{r}) = \frac{1}{2} G_{\alpha\beta}(r)\dot{r}^\alpha \dot{r}^\beta - \overline{V}(r), \tag{4}$$

where henceforth Greek indices will range from 1 to $m :=$dim $M = n-k$, the indices a, b, c will range from 1 to $k = dim\ G$, and where $\overline{V}\colon M \to \mathbb{R}$ is defined by $V = \overline{V} \circ \pi$. Since we will be dealing exclusively with the reduced constrained Lagrangian, we will drop the overbar on V henceforth. The $G_{\alpha\beta}$ are the components of the metric on the reduced space M induced by g according to $G_r(v_r, w_r) := g_q(\mathrm{hor}(v_q), \mathrm{hor}(w_q))$, where $r = \pi(q)$.

To arrive at the local equations of motion of a Chaplygin nonholonomic system we pick a local trivialization, where $Q = Q/G \times G$ and the action of G is given by left translation on the second factor, and choose coordinates r for the first factor and a basis e_a of the Lie algebra $\mathfrak{g}$ of G. The equations of motion then consist of a system of second-order ordinary differential equations on M, together with a system of first-order constraint equations [1]:

$$\frac{d}{dt}\frac{\partial l_c}{\partial \dot{r}^\alpha} - \frac{\partial l_c}{\partial r^\alpha} = -\left(\frac{\partial l}{\partial \xi^a}\right)^* \mathcal{B}^a_{\alpha\beta}\dot{r}^\beta, \tag{5}$$

$$\xi^a = -\mathcal{A}^a_\alpha(r)\dot{r}^\alpha. \tag{6}$$

Here the star indicates that we have substituted the constraints (6) into (5) *after* differentiation, and

$$\mathcal{B}^a_{\alpha\beta} = \frac{\partial \mathcal{A}^a_\beta}{\partial r^\alpha} - \frac{\partial \mathcal{A}^a_\alpha}{\partial r^\beta} - C^a_{bc}\mathcal{A}^b_\alpha \mathcal{A}^c_\beta \tag{7}$$

are the components of the curvature of $\mathcal{A}$, where C^a_{bc} are the structure constants of the Lie algebra defined by $[e_a, e_b] = C^a_{bc}$.

As discussed in the Introduction, the full equations of motion, (5)-(6), *cannot in general* be derived from Hamilton's principle [1, 17, 22]. In other words, nonholonomic mechanics is *not variational*, or said yet another way, (5)-(6) are not the Euler-Lagrange equations for any Lagrangian, or of the canonical Hamiltonian equations for any Hamiltonian (unless of course $\mathcal{B}^a_{\alpha\beta} = 0$, in which case the system in actually holonomic)[2].

2. Geometric integrators.

As discussed in the Introduction, the discretization of Hamilton's principle produces a variational integrator while discretizing the Lagrange-d'Alembert principle produces a nonholonomic integrator. Let us briefly review these discretizations.

2.1. Variational integrators.

Suppose that one is interested in simulating the dynamics of a Hamiltonian system between the two times $t = a$ and $t = b$. Begin by specifying the time steps $a = t_0 < t_1 < \ldots < t_N = b$ with fixed step size $h := t_{i+1} - t_i$, $i = 0, \ldots, N-1$, and define the discrete trajectory to be the sequence $q^j_0, \ldots, q^j_N \in Q$, $j = 1, \ldots, n$, where $q^j_i \approx q^j(t_i)$. Then, define the smooth map

[2]We should mention, however, that the full system (5)-(6) can in some cases be embedded, in a non-trivial way, in a larger system which *is* variational [14, 2].

$L_d\colon Q \times Q \to \mathbb{R}$ which will approximate the action over each time step[3]:

$$L_d(q_i, q_{i+1}) \approx \int_{t_i}^{t_{i+1}} L(q(t), \dot{q}(t))\, dt. \tag{8}$$

One can then define the *discrete action sum* $S_d(q_0, \ldots, q_N)$ by:

$$S_d(q_0, \ldots, q_N) = \sum_{i=0}^{N-1} L_d(q_i, q_{i+1}) \approx \int_a^b L(q(t), \dot{q}(t))\, dt. \tag{9}$$

Then, taking variations of the discrete path (with fixed endpoints) leads to the *discrete Euler-Lagrange* (DEL) equations [27]:

$$D_1 L_d(q_i, q_{i+1}) + D_2 L_d(q_{i-1}, q_i) = 0, \quad i = 1, \ldots, N-1, \tag{10}$$

where D_1, D_2 denote differentiation with respect to the first and second arguments, respectively, and where $q = (q^1, \ldots, q^n)$ on Q. The DEL equations (10), under appropriate regularity assumptions (see Section 7.2 in [8]), define the discrete time evolution of the system via the map $\Phi^v\colon Q \times Q \to Q \times Q$ given by $\Phi^v(q_{i-1}, q_i) = (q_i, q_{i+1})$ (where the superscript reminds us that this is a variational integrator algorithm). The explicit formula for Φ^v is only available when the DEL algorithm (10) is "explicit," in the sense that one can explicitly solve for $q_{i+1} = F(q_{i-1}, q_i))$. This happens, for example, when the Lagrangian L has a constant kinetic energy metric g [27]. Otherwise, the algorithm (10) will be implicit, and one must use implicit numerical solvers (such as a Newton method) to implement it.

One can show that the algorithm Φ^v preserves the discrete canonical symplectic form

$$\Omega_{L_d}(q_0, q_1) = \frac{\partial^2 L_d}{\partial q_0^i \partial q_1^j} dq_0^i \wedge dq_1^j. \tag{11}$$

Moreover, provided the discrete Lagrangian is invariant under the action of G on Q, the algorithm also preserves the discrete momentum map $J_d\colon Q \times Q \to \mathfrak{g}^*$ given by

$$\langle J_d(q, q'), \xi \rangle = \langle D_2 L_d(q, q'), \xi_Q(q') \rangle; \tag{12}$$

for details see [27] (Section 1.3.2 and Theorem 1.3.3).

Now, although L admits many discretizations, we will restrict ourselves here to *symmetrized discrete Lagrangians*

$$L_d^{sym,\epsilon}(q_i, q_{i+1}) = \frac{1}{2}\left(L_d^{\epsilon}(q_i, q_{i+1}) + L_d^{1-\epsilon}(q_i, q_{i+1})\right), \tag{13}$$

$$\text{where} \quad L_d^{\epsilon}(q_i, q_{i+1}) := hL\left((1-\epsilon)q_i + \epsilon q_{i+1}, \frac{q_{i+1} - q_i}{h}\right).$$

The reason for using this particular discretization is that it produces second-order variational integrators for any $\epsilon \in [0, 1]$; see Section 2.3 of [27].

[3]We will choose the same discretization for each time interval $[t_i, t_{i+1}]$. Although one can certainly drop this restriction (see [27]), for simplicity we will continue using this assumption henceforth.

2.2. **Nonholonomic integrators.** The discretization of nonholonomic mechanics begins again with the discrete Lagrangian L_d, but now adds a discrete constraint space $\mathcal{D}_d \subset Q \times Q$ having the same dimension as $\mathcal{D}$, and containing the diagonal: $(q, q) \in \mathcal{D}_d$ for all $q \in Q$. The solution sequence $\{q_i\}$ is then restricted by $(q_i, q_{i+1}) \in \mathcal{D}_d$ through the discretization of the constraint one-forms ω^a which define $\mathcal{D}$:

$$\omega_d^{a,\epsilon,sym}(q_i, q_{i+1}) = \frac{1}{2}\left(\omega_d^{a,\epsilon}(q_i, q_{i+1}) + \omega_d^{a,1-\epsilon}(q_i, q_{i+1})\right), \tag{14}$$

$$\begin{aligned}\omega_d^{a,\epsilon}(q_i, q_{i+1}) &:= \omega^a\left((1-\epsilon)q_i + \epsilon q_{i+1}, \frac{q_{i+1}-q_i}{h}\right)\\ &= c_j^a\left((1-\epsilon)q_i + \epsilon q_{i+1}\right)\frac{q_{i+1}-q_i}{h}.\end{aligned}$$

The $\omega_d^{a,\epsilon} : Q \times Q \to \mathbb{R}$, $a = 1, \dots, k$, are the functions whose annihilation defines $\mathcal{D}_d$, meaning that $(q_i, q_{i+1}) \in \mathcal{D}_d$ if and only if $\omega_d^{a,\epsilon}(q_i, q_{i+1}) = 0$.

Taking variations of the discrete action (9) (with fixed endpoints) and enforcing the conditions $\delta q_i \in \mathcal{D}_{q_i}$, along with $(q_i, q_{i+1}) \in \mathcal{D}_d$, yields the *discrete Lagrange-d'Alembert* (DLA) algorithm [9]:

$$D_1 L_d(q_i^j, q_{i+1}^j) + D_2 L_d(q_{i-1}^j, q_i^j) = \lambda_a c_j^a(q_i), \tag{15}$$

$$\omega_d^a(q_i^j, q_{i+1}^j) = 0. \tag{16}$$

Here L_d, ω_d^a are unsymmetrized, $\epsilon = 0$, and λ_a are Lagrange multipliers.

We will also refer to (15)-(16) as the *nonholonomic integrator*, and will denote the discrete time evolution map it defines by Φ^{nh}. We remark that, as pointed out in Section 7.3 of [8], one should apply the same discretization technique for both L and ω^a, meaning that if L is symmetrized according to (13), then the ω^a should be symmetrized according to (14).

Example: As our running example, let us consider the motion of a free particle in $Q = \mathbb{R}^3$ subjected to a particular nonholonomic constraint—the so-called "nonholonomic" free particle [1]. Supposing the particle has unit mass, the Lagrangian and constraint are given by:

$$L = \frac{1}{2}\left(\dot{x}^2 + \dot{y}^2 + \dot{z}^2\right), \qquad \dot{z} + x\dot{y} = 0. \tag{17}$$

For this system, $q = (x, y, z)$, $n = 3$, $k = 1$, $c_1^1 = c_3^1 = 0$ and $c_2^1 = x$. The discrete Lagrangian $L_d^\epsilon(q_i^j, q_{i+1}^j)$ and discrete constraint $\omega_d^\epsilon(q_i^j, q_{i+1}^j)$ are given by:

$$L_d^\epsilon(q_i^j, q_{i+1}^j) = \frac{h}{2}\left(\left(\frac{x_{i+1}-x_i}{h}\right)^2 + \left(\frac{y_{i+1}-y_i}{h}\right)^2 + \left(\frac{z_{i+1}-z_i}{h}\right)^2\right), \tag{18}$$

$$\omega_d^\epsilon(q_i^j, q_{i+1}^j) = \frac{z_{i+1}-z_i}{h} + \left((1-\epsilon)x_i + \epsilon x_{i+1}\right)\left(\frac{y_{i+1}-y_i}{h}\right). \tag{19}$$

Returning to the theory, we note that the DLA algorithm is designed to approximate the discrete trajectory for the *full* nonholonomic problem (reduced mechanics together with constraint kinematics). However, Chaplygin Hamiltonization, discussed in Section 3, is performed on the reduced system (5). The resulting nonholonomic integrator which discretizes the reduced mechanics leads to the *reduced discrete Lagrange-d'Alembert algorithm* (RDLA).

Following [8] (Section 7.5.3), one begins by noting that locally Q can be identified with $M \times G$, which we will coordinatize by $q_i = (r_i, g_i)$. Moreover, the

discretized constraints (16) allow $\mathcal{D}_q$ to be identified with $M \times M \times G$ locally through $(r_i, g_i, r_{i+1}, g_{i+1}) \in \mathcal{D}_q \to (r_i, r_{i+1}, g_i)$ since g_{i+1} is uniquely determined by the discretized constraint forms $\omega_d^{a,\epsilon}(r_i, g_i, r_{i+1}, g_{i+1}) = 0$. Then we can define $L_d^c \colon \mathcal{D}_q \to \mathbb{R}$, the restriction of the discrete Lagrangian L_d to $\mathcal{D}_q$. This leads to the reduced discrete Lagrangian $L_d^* \colon M \times M \to \mathbb{R}$ defined by

$$L_d^*(r_k, r_{k+1}) = L_d^c(r_k, r_{k+1}, e). \tag{20}$$

The DLA algorithm then reduces to the RDLA algorithm on M (see Section 7.5.3 of [8]):

$$D_1 L_d^*(r_i^\alpha, r_{i+1}^\alpha) + D_2 L_d^*(r_{i-1}^\alpha, r_i^\alpha) = F^-(r_i^\alpha, r_{i+1}^\alpha) + F^+(r_{i-1}^\alpha, r_i^\alpha), \tag{21}$$

where F^+, F^- are the discretizations of the right-hand-side force in (5) (see Section 7.5.3 of [8] for more details):

$$\begin{aligned} F^-(q_i, q_{i+1}) &= \frac{\partial l_d}{\partial f_{i,i+1}}(r_i, r_{i+1}, f_{i,i+1}) \frac{\partial g_{i+1}}{\partial r_i^\beta}(r_i, r_{i+1}) e_b \\ &\quad - R^*_{f_{i,i+1}} \frac{\partial l_d}{\partial f_{i,i+1}}(r_i, r_{i+1}, f_{i,i+1}) \mathcal{A}_\beta^b(r_i) e_b, \end{aligned} \tag{22}$$

$$\begin{aligned} F^+(q_{i-1}, q_i) &= \frac{\partial l_d}{\partial f_{i-1,i}}(r_{i-1}, r_i, f_{i-1,i}) \frac{\partial g_i}{\partial r_i^\beta}(r_{i-1}, r_i) e_b \\ &\quad + U^*_{g_i(r_{i-1}, r_i)} \frac{\partial l_d}{\partial f_{i-1,i}}(r_{i-1}, r_i, f_{i-1,i}) \mathcal{A}_\beta^b(r_i) e_b, \end{aligned} \tag{23}$$

$$f_{i,i+1} = g_i^{-1} g_{i+1} = g_{i+1}(r_i, r_{i+1}), \quad l_d(r_i, r_{i+1}, f_{i,i+1}) = L_d(r_i, e, r_{i+1}, g_i^{-1} g_{i+1}).$$

Here R_g, U_g denote right and left multiplication in the Lie group by $g \in G$, and $\{e_b\}$ is a basis for $\mathfrak{g}$. We will also symmetrize the RDLA, as in (13) in what follows, and indicate that by the ϵ, sym superscript. In addition, if we denote the right-hand-side of (5) by $F_\alpha(r, \dot{r})$, then for $\mathfrak{g}$ abelian, as in the case of the classical Chaplygin systems where $G = \mathbb{R}^i \times \mathbb{T}^{k-i}$, the (symmetrized) discrete forces become

$$F_\alpha^{-,sym,\epsilon}(q_{i-1}, q_i) = \frac{1}{2}\left(F_\alpha^\epsilon(r_{i-1}, r_i) + F_\alpha^{1-\epsilon}(r_{i-1}, r_i)\right), \tag{24}$$

$$F_\alpha^{+,sym,\epsilon}(q_i, q_{i+1}) = \frac{1}{2}\left(F_\alpha^\epsilon(r_i, r_{i+1}) + F^{1-\epsilon}(r_i, r_{i+1})\right), \tag{25}$$

$$\text{where} \quad F_\alpha^\epsilon(r_i, r_{i+1}) = F_\alpha\left((1-\epsilon) r_i + \epsilon r_{i+1}, \frac{r_{i+1} - r_i}{h}\right).$$

Example: To continue our example, we first note that the system (17) is abelian Chaplygin since it is translationally invariant in the z-direction, so that $G = \mathbb{R}$. Thus we have $r = (x, y)$, $g = z$, $q = (x, y, z)$, and the resulting constrained Lagrangian is:

$$l_c(r, \dot{r}) = \frac{1}{2}\left(\dot{x}^2 + (1 + x^2)\dot{y}^2\right). \tag{26}$$

Now, with $\mathcal{A}_y^z = x$, a simple computation shows that $\mathcal{B}_{xy}^z = -1$ is the only non-zero curvature component. Thus, the constraint reaction forces F_1, F_2, and their discretizations are given by:

$$F_1 = -x\dot{y}^2, \quad F_2 = x\dot{y}^2, \quad F_\alpha^\epsilon = \pm h\left((1-\epsilon)x_i + \epsilon x_{i+1}\right)\left(\frac{y_{i+1} - y_i}{h}\right)^2, \tag{27}$$

where F_2^ϵ carries the positive sign and F_1^ϵ the negative one. Moreover, the discrete constrained Lagrangian $L_d^{*,\epsilon}(r_i^j, r_{i+1}^{j+1})$ (20) is given by

$$L_d^{*,\epsilon}(r_i^j, r_{i+1}^j) = \frac{h}{2}\left[\left(\frac{x_{i+1}-x_i}{h}\right)^2 + \Big(1+((1-\epsilon)x_i+\epsilon x_{i+1})^2\Big)\left(\frac{y_{i+1}-y_i}{h}\right)^2\right], \tag{28}$$

which is just the discretization of (26).

Like the variational integrator, the DLA and RDLA nonholonomic integrators have geometric invariance properties. In the continuous setting, under the action of a Lie group G on Q which leaves L and $\mathcal{D}$ invariant, the associated momentum map J is in general not conserved. Instead, along the integral curves of the nonholonomic equations, it satisfies a nonholonomic momentum equation [1] (Section 5.5). If this invariance passes to the discrete setting, so that $L_d, \mathcal{D}_d$ are again invariant under the action of G on Q, then the DLA and RDLA algorithms satisfy a discrete version of the nonholonomic momentum equation [8] (Section 7.5). In addition, the two algorithms also preserve the discrete evolution of the canonical symplectic form under the nonholonomic flow [9] (Section 5). Thus, these nonholonomic integrators *are not variational integrators*, meaning that they do not follow from a discretization of Hamilton's principle. It would seem then that applying variational integrators to simulate nonholonomic systems would be impossible.

3. **Chaplygin Hamiltonization.**

As noted in the Introduction, the reduced mechanics of *Chaplygin Hamiltonizable* nonholonomic systems are Hamiltonian after a suitable reparameterization of time. Let us now discuss this in more detail.

Suppose that a two degree of freedom ($dim\ M = 2$) nonholonomic Chaplygin system possesses an invariant measure with density $f(r_1, r_2)$, meaning that the Lie derivative of the two form $f\Omega$ along the nonholonomic flow vanishes, where Ω is the canonical symplectic form on T^*M. Then, in [7] it was shown that the reduced equations of motion (5) are Hamiltonian in the new time defined by the reparameterization $d\tau = f(r_1, r_2)\, dt$. Moreover, it also follows that if a nonholonomic system can be written in Hamiltonian form after the time reparameterization $d\tau = f(r)\, dt$, then the original system has an invariant measure with density $f(r)^{m-1}$, [10], where $m = dim\ M$. As mentioned in the Introduction, these two results are collectively known as Chaplygin's Reducibility Theorem, and the function f is known as the *reducing multiplier*, or simply the *multiplier*; see [10] and references therein. If f has zeros, then the results only hold locally on open subsets of M.

Chaplygin's Theorem has been expanded and generalized beyond the two degree of freedom case, [15], and the process of finding a Hamiltonian form for the reduced mechanics of a nonholonomic system via a reparameterization of time is now called *Chaplygin Hamiltonization*[4]. Fortunately, the class of Chaplygin Hamiltonizable nonholonomic systems is large (see Tables 1 and 2 in [3], [4], and [15] for a list of examples), and, given a nonholonomic system, one can check its Chaplygin Hamiltonizability directly by solving a system of first-order linear partial differential equations for f, [15] (Theorem 1). For Chaplygin systems, the relevant equations depend on the metric G and curvature $\mathcal{B}$.

[4]There are other methods of Hamiltonizing a nonholonomic system which do not require a time reparameterization, see [12]

Once the Chaplygin Hamiltonization has been achieved, one then has a Hamiltonian system (relative to the reparameterized time τ) to which one can apply any of the known techniques applicable to Hamiltonian systems. In particular, one can now simulate the dynamics of this (Hamiltonized) system and then "undo" the Hamiltonization to arrive at a simulation of the reduced mechanics of the original Chaplygin system. Let us now give the details.

4. **Variational integrators for Chaplygin Hamiltonizable nonholonomic systems.** For the remainder of this section, suppose that we have already succeeded in Chaplygin Hamiltonizing a Chaplygin system. Then, by the chain rule we have

$$r'(\tau) = \frac{dr}{d\tau}(\tau) = \frac{1}{f(r(t(\tau)))}\dot{r}(t(\tau)).$$

Using this we can define the reduced constrained Hamiltonized Lagrangian

$$\mathcal{L}_c(r, r') := l_c(r, \dot{r} = f(r)r') = \frac{1}{2}f(r)^2 G_{\alpha\beta}(r) r'^{\alpha} r'^{\beta} - V(r).$$

Supposing that $\mathcal{L}_c$ is regular, then we can define the momenta $P = \partial\mathcal{L}_c/\partial r'$ and the "Hamiltonized Hamiltonian" $\mathcal{H}_c(r, P)$ via the usual Legendre transform. We can now apply a variational integrator to our Hamiltonized system, and then undo the Hamiltonization to arrive at approximations for the actual reduced nonholonomic trajectories. However, doing so requires the discretization of the inverse transformation $\tau \mapsto t$ given by:

$$t(\tau) = \int_0^{\tau} \frac{1}{f(r(\tilde{\tau}))}\, d\tilde{\tau}, \tag{29}$$

where we have set, without loss of generality, $t_0 = \tau_0 = 0$, and where hereafter we shall assume $f \neq 0$, unless otherwise noted. We shall discuss the discretization of (29) in Section 4.1 below, but note briefly here the obvious: such a quadrature rule will introduce an error δt_i, producing $r^{\alpha}(t_i + \delta t_i)$ as the approximation for $r^{\alpha}(t_i)$ For this reason, in Section 4.2 below we will introduce an alternative method which does not require that one invert the transformation, thus avoiding this error. However, there we shall see that other challenges arise.

Example: Returning to our running example, one can show that the nonholonomic free particle is a Chaplygin Hamiltonizable system, with f given by $f(x) = (1 + x^2)^{-1/2}$ [15]. The time reparameterization $d\tau = f(x)\, dt$ then leads to $x' = (1+x^2)\dot{x}$ and $y' = (1 + x^2)\dot{y}$, and the Hamiltonized Lagrangian is given by

$$\mathcal{L}_c(r, r') = \frac{1}{2}\left[\frac{x'^2}{1 + x^2} + y'^2\right], \quad \text{where} \quad r = (x, y). \tag{30}$$

This Lagrangian is regular, and by calculating the momenta

$$P_x = (1 + x^2)^{-1/2}x', \quad P_y = y',$$

the Hamiltonized Hamiltonian corresponding to (30) is

$$\mathcal{H}_c(r, P) = \frac{1}{2}\left[(1 + x^2)P_x^2 + P_y^2\right]. \tag{31}$$

4.1. **Integrators via time reparameterization.** First, let us begin by defining the symmetrized discrete Hamiltonized Lagrangian $\mathcal{L}_c^{sym,\epsilon}$ from (13):

$$\mathcal{L}_d^{sym,\epsilon}(r_i, r_{i+1}) = \frac{1}{2}\left(\mathcal{L}_d^{\epsilon}(r_i, r_{i+1}) + \mathcal{L}_d^{1-\epsilon}(r_i, r_{i+1})\right), \tag{32}$$

$$\text{where} \quad \mathcal{L}_d^{\epsilon}(r_i, r_{i+1}) := h_\tau \mathcal{L}_c\left((1-\epsilon)r_i + \epsilon r_{i+1}, \frac{r_{i+1}-r_i}{h_\tau}\right), \ h_\tau := \tau_{i+1} - \tau_i.$$

We can then apply the DEL algorithm (10) to arrive at our first new integrator.

Definition 4.1. The Hamiltonized discrete Euler-Lagrange equations (HDEL) are defined by

$$D_1\mathcal{L}_d^{sym,\epsilon}(r_i, r_{i+1}) + D_2\mathcal{L}_d^{sym,\epsilon}(r_{i-1}, r_i) = 0, \quad i = 1, \dots, N_\tau - 1, \tag{33}$$

where N_τ is the total number of iterations.

These discrete equations approximate the trajectories according to $r^\alpha(\tau_i) \approx r_i^\alpha$. However, to compare to the RDLA algorithm (21) we need to calculate the discrete t-values from the discrete τ-values according to

$$t_i = \int_0^{\tau_i} F(r(\tilde{\tau}))\, d\tilde{\tau}, \quad i = 0, \dots, N_\tau, \quad \text{where} \quad F(r(\tilde{\tau})) := \frac{1}{f(r(\tilde{\tau}))}. \tag{34}$$

This requires that we apply a quadrature rule to each integral in (34). For simplicity, we will choose to apply the same Newton-Cotes quadrature rule to each integral[5]. The simplest of such rules is the trapezoidal rule, which yields the approximations:

$$t_i \approx \begin{cases} \dfrac{h_\tau}{2}\left(F(0) + F(\tau_1)\right), & i = 1, \\ \dfrac{h_\tau}{2}\left(F(0) + F(\tau_i) + 2\displaystyle\sum_{l=1}^{i-1} F(l h_\tau)\right), & i = 2, \dots, N_\tau. \end{cases} \tag{35}$$

These approximations produce an error δt_i in the assignment of a t-value to each τ-value that the HDLA algorithm (33) uses. More specifically, we have the following.

Proposition 1. *Suppose that there exist $C_i \in \mathbb{R}$, $i = 1, \dots, N_\tau$ such that $|F''(r(\tau))| \leq C_i$ for all $\tau \in (\tau_{i-1}, \tau_i)$. Then the errors δt_i in making the approximations (35) are bounded by*

$$|\delta t_i| \leq \frac{h_\tau^3}{12}\sum_{l=1}^{i} C_l, \qquad i = 1, \dots, N_\tau. \tag{36}$$

Proof. We can write the integral (34) as

$$t_i = \sum_{l=1}^{i}\int_{\tau_{l-1}}^{\tau_l} F(r(\tilde{\tau}))\, d\tilde{\tau}, \qquad i = 1, \dots, N_\tau. \tag{37}$$

It is well known that there exist $\eta_{i-1,i} \in (\tau_{i-1}, \tau_i)$ such that the error Δt_i in approximating the integral $\int_{\tau_{i-1}}^{\tau_i} F(r(\tilde{\tau}))\, d\tilde{\tau}$ by the trapezoidal rule is given by

$$\Delta t_i = -\frac{h_\tau^3}{12} F''(\eta_{i-1,i}). \tag{38}$$

[5]Since we require the timestep to be fixed, we will not discuss the application of Gaussian quadrature formulas. Although Gaussian quadrature gives better accuracy for a given order, the non-constant timesteps it requires would necessitate the usage of asynchronous variational integrators.

Therefore, approximating each integral in (37) by the trapezoidal rule produces the *global error* (see Theorem 7.16 in [16])

$$\delta t_i = -\frac{h_\tau^3}{12}\sum_{l=1}^{i} F''(\eta_{l-1,l}), \qquad i = 1, \dots, N_\tau. \tag{39}$$

The claim then follows from the hypotheses on $F''(r)$. □

Thus, due to Proposition 1, although the HDLA algorithm (33) produces second-order approximations to $r^\alpha(\tau_j)$, when converted to t-time this yields the second-order approximation $r^\alpha(t_j + \delta t_j)$ to $r^\alpha(t_j)$. We note that one could decrease the error δt_i by using a higher-order Newton-Cotes formula, like Simpson's or Boole's rule, but for simplicity we will only discuss the trapezoidal rule here.

Remark 1: In practice, since we are using the HDEL algorithm to compute second-order approximations to $r^\alpha(\tau_i)$, we will not have *a priori* an explicit expression for $r^\alpha(\tau)$ with which we can compute the bounds C_i. Instead, we must first express r'' as a function of r, r' through the Euler-Lagrange equations for $\mathcal{L}_c$, so that $(r^\alpha)'' = g^\alpha(r, r')$. Then, after differentiating $F''(r(\tau))$ with the chain rule, we can write $F''(r(\tau)) = g(r, r', r'') = g(r, r'))$. We can then finally use the discrete trajectory values r_i^α computed from the HDEL algorithm to find the bounds C_i. We will illustrate this in Section 5 below.

Let us note that although the HDLA uses the constant step size h_τ, for $f \neq const.$ the corresponding step size $h_i = t_{i+1} - t_i$ varies once the approximations (37) are made. Although this is a shortcoming of this method, if one is merely interested in the geometry of the trajectories, then one can avoid the approximations (37) altogether by choosing one of the r^α as a new independent variable and plotting (in τ-time) the other r^β against it. We shall illustrate this strategy in Section 5 below.

Given some of the difficulties presented by the need to approximate the integrals (34), we will discuss an alternative method which avoids the need to invert the time transformation altogether in the next section. Before doing so, let us illustrate the discretization (32).

Example: Returning to our running example, we discretize the Hamiltonized Lagrangian (30) by first computing $\mathcal{L}_d^\epsilon$:

$$\mathcal{L}_d^\epsilon(r_i, r_{i+1}) = \frac{h_\tau}{2}\left[\frac{1}{1 + ((1-\epsilon)x_i + \epsilon x_{i+1})^2}\left(\frac{x_{i+1} - x_i}{h_\tau}\right)^2 + \left(\frac{y_{i+1} - y_i}{h_\tau}\right)^2\right], \tag{40}$$

and then computing $\mathcal{L}_d^{sym,\epsilon}$ according to (32). Then, the HDEL equations follow from (33), where $r = (x, y)$. Numerical results will follow in Section 5.1.

4.2. **Integrators via Poincaré transformations.** The time reparameterization $d\tau = f(r)\, dt$, apart from its usage in the Hamiltonization of nonholonomic systems, is also well-known from the theory of adaptive geometric integrators. In fact, in Chapter 9 of [23] the reparameterization is called a *Sundman transformation*, and has been used in computational astronomy to vary an integrator's timestep[6]. An alternative which achieves the same objective is known as a *Poincaré transformation* [23] (Chapter 9).

[6] As [19] notes, this nomenclature dates back to Levi-Civita's treatment of the three body problem.

To construct this transformation, we follow Section 9.1 of [23], and first define the Hamiltonian $\tilde{\mathcal{H}}_c(r,P) := f(r)\left(\mathcal{H}_c(r,P) - E\right)$, where $E := \mathcal{H}_c(r^0,P_0)$. We can then view $r(\tau), P(\tau), \tilde{\mathcal{H}}_c$ as functions of t via (29). The canonical equations of motion for $\tilde{\mathcal{H}}_c$, written in terms of $\mathcal{H}_c$, are

$$\frac{dr^\alpha}{dt} = f(r)\frac{\partial \mathcal{H}_c}{\partial P_\alpha}, \tag{41}$$

$$\frac{dP_\alpha}{dt} = -f(r)\frac{\partial \mathcal{H}_c}{\partial r^\alpha} - \left(\mathcal{H}_c(r,P) - E\right)\frac{\partial f}{\partial r^\alpha}. \tag{42}$$

Now, since the system (41)-(42) is Hamiltonian, $\tilde{\mathcal{H}}_c$ is conserved in time, and in particular equal to its initial value, so that $\tilde{\mathcal{H}}_c(r(t),P(t)) = \tilde{\mathcal{H}}_c(r(0),P(0)) = f(r)\left(\mathcal{H}_c(r(0),P(0)) - E\right)$. If we now choose the initial conditions $r(0) = r^0, P(0) = P_0$, then $\tilde{\mathcal{H}}_c(r^0,P_0) = 0$, and hence $\tilde{\mathcal{H}}_c(r(t),P(t)) = 0$, which gives $\mathcal{H}_c(r(t),P(t)) = E$. With this choice of initial conditions the parenthetical term in (42) vanishes and the system (41)-(42) reduces to the system

$$\frac{dr^\alpha}{dt} = f(r)\frac{\partial \mathcal{H}_c}{\partial P_\alpha}, \quad \frac{dP_\alpha}{dt} = -f(r)\frac{\partial \mathcal{H}_c}{\partial r^\alpha}. \tag{43}$$

This is significant because in Section 4 we defined the Hamiltonian $\mathcal{H}_c(r,P)$ from $\mathcal{L}_c(r,r')$ according to $\mathcal{H}_c(r,P) = r'^\alpha P_\alpha - \mathcal{L}_c(r,r')$. By using $d\tau = f(r)\,dt$ and the chain rule to rewrite r', P', as well as (29), the canonical equations of motion of $\mathcal{H}_c$ are transformed into precisely (43). Thus, *the non-Hamiltonian system* (43) *can be represented as the Hamiltonian system* (41)-(42) *provided we choose the initial conditions such that* $\tilde{\mathcal{H}}_c(r^0,P_0) = 0$. More precisely, one can easily show that given the same initial condition the solutions to (41)-(42) and (43) are identical, up to the reparameterization (29) [19] (Lemma 1).

To apply the Poincaré transformation in practice, one chooses the initial conditions $r(0), P(0)$ and *then* constructs $\tilde{\mathcal{H}}_c(r,P)$ by inserting the value $E = \mathcal{H}_c(r^0,P_0)$. Before proceeding to the discretization of the system (41)-(42), let us first find the corresponding Lagrangian $\tilde{\mathcal{L}}_c$ (since we will need it to apply the DEL algorithm).

Proposition 2. *The Poincaré Lagrangian* $\tilde{\mathcal{L}}_c(r,\dot{r})$ *is given by*

$$\tilde{\mathcal{L}}_c(r,\dot{r}) = f(r)\left(l_c(r,\dot{r}) + E\right) = \frac{f(r)}{2}G_{\alpha\beta}(r)\dot{r}^\alpha\dot{r}^\beta - f(r)(V(r) - E). \tag{44}$$

Proof. By definition, we have

$$\begin{aligned}
\tilde{\mathcal{L}}_c(r,\dot{r}) &= \dot{r}^\alpha P_\alpha - \tilde{\mathcal{H}}_c(r,\dot{r}) \\
&= \dot{r}^\alpha(f(r)G_{\alpha\beta}(r)\dot{r}^\beta) - f(r)\left(\frac{1}{2(f(r))^2}G_{\alpha\beta}(r)(f(r))^2\dot{r}^\alpha\dot{r}^\beta + V(r) - E\right) \\
&= \frac{f(r)}{2}G_{\alpha\beta}(r)\dot{r}^\alpha\dot{r}^\beta - f(r)(V(r) - E) = f(r)\left(l_c(r,\dot{r}) + E\right).
\end{aligned} \tag{45}$$

□

We can then define the symmetrized discrete Poincaré transformed Hamiltonized Lagrangian $\tilde{\mathcal{L}}_d^{sym,\epsilon}(r_i,r_{i+1})$ by (32), where we replace $\mathcal{L}_c$ by $\tilde{\mathcal{L}}_c$ from (44), and h_τ by h. We can then apply the DEL algorithm (10) to arrive at our second integrator.

Definition 4.2. The Poincaré transformed Hamiltonized discrete Euler-Lagrange equations (PTHDEL) are defined by

$$D_1\tilde{\mathcal{L}}_d^{sym,\epsilon}(r_i, r_{i+1}) + D_2\tilde{\mathcal{L}}_d^{sym,\epsilon}(r_{i-1}, r_i) = 0, \qquad i = 1, \dots, N-1. \tag{46}$$

The algorithm (46) proceeds in discretized t-time, versus the algorithm (33) which proceeds in discretized τ-time. Thus, (46) has the advantage of avoiding the problematic discretization of (29) in order to recover the t-time approximations from (33). However, the discrete energy behavior of the algorithm (46) depends on $f(r)$. To see this, we note that for a general regular Lagrangian L, its associated energy function $E_L(t)$ is defined by

$$E_L(t) = \dot{r}^\alpha \frac{\partial L}{\partial \dot{r}^\alpha} - L(r(t), \dot{r}(t)), \tag{47}$$

and for the Lagrangians l_c and $\tilde{\mathcal{L}}_c$ we have

$$E_{l_c}(t) = l_c(r(t), \dot{r}(t)) + 2V(r(t)), \tag{48}$$

$$E_{\tilde{\mathcal{L}}_c}(t) = f(r(t))\left(l_c(r(t), \dot{r}(t)) + 2V(r(t)) - E\right) = f(r(t))(E_{l_c}(t) - E) \tag{49}$$

From (49) it follows immediately that

$$E_{l_c}(t) = E + F(r(t))E_{\tilde{\mathcal{L}}_c}, \tag{50}$$

where we remind the reader that $F(r) = (f(r))^{-1}$.

In the continuous case, since the chosen initial conditions result in $\tilde{\mathcal{H}}_c = 0 = E_{\tilde{\mathcal{L}}_c}$ for all t (as discussed following the system (43)), it follows from (50) that the energy of the constrained reduced nonholonomic mechanics E_{l_c} is conserved. Once we discretize $\tilde{\mathcal{L}}_c$, like any fixed timestep variational integrator the PTHDEL algorithm (46) will not exactly conserve the discrete energies $(E_{\tilde{\mathcal{L}}_c})_d(r_i, r_{i+1})$. By (50), the deviations in $E_{l_c} - E$ at each timestep, as [23] (pg. 237) points out, will depend on f. If f is bounded or grows (so that F is bounded or decays) we expect the PTHDEL algorithm to inherit the good long-term behavior of the discrete energies $(E_{\tilde{\mathcal{L}}_c})_d$. We will see this in Section 5.

Example: Let us now illustrate the Poincaré transformation for our running example. Using the reduced constrained Lagrangian (26) we can define the Poincaré transformed Lagrangian $\tilde{\mathcal{L}}_c$ from (44) by:

$$\tilde{\mathcal{L}}_c(r, \dot{r}) = \frac{1}{2}\left[\frac{\dot{x}^2}{\sqrt{1+x^2}} + \sqrt{1+x^2}\,\dot{y}^2\right] + \frac{E}{\sqrt{1+x^2}}. \tag{51}$$

We then construct the symmetrized discrete Lagrangian corresponding to (51) according to (32), where $\tilde{\mathcal{L}}_d^\epsilon$ is given by:

$$\begin{aligned}\tilde{\mathcal{L}}_d^\epsilon(r_i, r_{i+1}) &= \frac{h}{2\sqrt{1+((1-\epsilon)x_i + \epsilon x_{i+1})^2}}\left(\frac{x_{i+1}-x_i}{h}\right)^2 \\ &+ \frac{h}{2}\sqrt{1+((1-\epsilon)x_i + \epsilon x_{i+1})^2}\left(\frac{y_{i+1}-y_i}{h}\right)^2 \\ &+ \frac{E}{\sqrt{1+((1-\epsilon)x_i + \epsilon x_{i+1})^2}}.\end{aligned} \tag{52}$$

The PTHDEL algorithm then proceeds according to (46), where $r = (x, y)$.

Before proceeding to the examples, we have quickly summarized the three integrators we will be comparing in the next section and some of their properties in Tables 1 and 2 below.

Integrator	Algorithm
RDLA (21)	$D_1L_d^*(r_i, r_{i+1}) + D_2L_d^*(r_{i-1}, r_i) = F^-(r_i, r_{i+1}) + F^+(r_{i-1}, r_i)$
HDEL (33)	$D_1\mathcal{L}_d^{sym,\epsilon}(r_i, r_{i+1}) + D_2\mathcal{L}_d^{sym,\epsilon}(r_{i-1}, r_i) = 0$
PTHDEL (46)	$D_1\tilde{\mathcal{L}}_d^{sym,\epsilon}(r_i, r_{i+1}) + D_2\tilde{\mathcal{L}}_d^{sym,\epsilon}(r_{i-1}, r_i) = 0$

TABLE 1. Comparison of Integrator Formulations.

Integrator	Time Used	Variational?
Nonholonomic (21)	t	No
HDEL (33)	τ	Yes
PTHDEL (46)	t	Yes

TABLE 2. Comparison of Integrator Properties.

5. **Examples.**

5.1. **The nonholonomic particle.** Let us return to our running example, the nonholonomic free particle with unit mass. Before discussing the numerical results, let us remark that we have chosen to begin with this system since it is integrable by quadratures, and hence we can directly compare both of the integrators developed above (the HDEL and PTHDEL) to the exact solutions. The solutions to the constrained nonholonomic equations of motion (5) are given by [13]:

$$x(t) = \alpha_x t, \qquad y(t) = \frac{\alpha_y}{\alpha_x} \ln\left(x(t) + \sqrt{1 + x(t)^2}\right), \tag{53}$$

where we have chosen, without loss of generality, the initial conditions $x_0 = y_0 = 0$, and we have assumed that $\alpha_x := \dot{x}(0) \neq 0$ and $\alpha_y := \dot{y}(0) \neq 0$. Moreover, the time reparameterization is given explicitly by integrating $d\tau = (1 + x(t)^2)^{-1/2}\, dt$, using $x(t)$ from (53), to arrive at

$$\tau(t) = \frac{1}{\alpha_x} \ln\left(x(t) + \sqrt{1 + x(t)^2}\right), \tag{54}$$

where $\tau_0 = \tau(t = 0) = 0$. One can also invert (54) and find $t(\tau)$:

$$t(\tau) = \frac{1}{\alpha_x} \sinh\left(\alpha_x \tau\right), \quad \text{and also} \quad \tau(t) = \frac{1}{\alpha_x} \sinh^{-1}(\alpha_x t), \tag{55}$$

and as a consequence we can use $t(\tau)$ in (53) to arrive at the reduced dynamics in terms of τ:

$$x(\tau) = \sinh\left(\alpha_x \tau\right), \qquad y(\tau) = \alpha_y \tau. \tag{56}$$

From (56) it follows that

$$x = \sinh\left(\frac{\alpha_x}{\alpha_y} y\right), \tag{57}$$

which we will use to compare the performance of the two integrators developed above.

Let us now turn to the numerical simulations. We have chosen $\alpha_x = \alpha_y = 1$, $h = h_\tau = 0.05$ and $N = 200$. Thus, the simulation time hN is 10 seconds. With our choice of initial conditions the energy $E = 1$, and we will use the symmetrized versions of the Lagrangians (28), (52), and (40) with $\epsilon = 0.5$ as the symmetrization parameter. Also, since from (54) we see that $\tau(10) \approx 2.998$, then 200 iterations in t-time corresponds to $\tau(10)/h_\tau \approx 60$ iterations in τ-time. Thus, to more easily compare the nonholonomic (RDLA) and HDEL integrators, we will choose $N_\tau = 60$. We also wish to note that all of our numerical calculations were done using MAPLE.

Figure 1 below shows a comparison of the root mean square deviation (rmsd) of the discrete values computed by each algorithm from the known solutions (53) for the RDLA and PTHDEL algorithms and (56) for the HDEL algorithm. This error is defined by $\sqrt{(x_i - x(t_i))^2 + (y_i - y(t_i))^2}$ for the RDLA and PTHDEL algorithms, and an analogous expression, with t replaced by τ for the HDEL algorithm. The rmsd error is smallest for the RDLA algorithm (of order 10^{-4}), followed by the HDEL algorithm (of order 10^{-3}) and finally the PTHDEL algorithm (of order 10^{-2}).

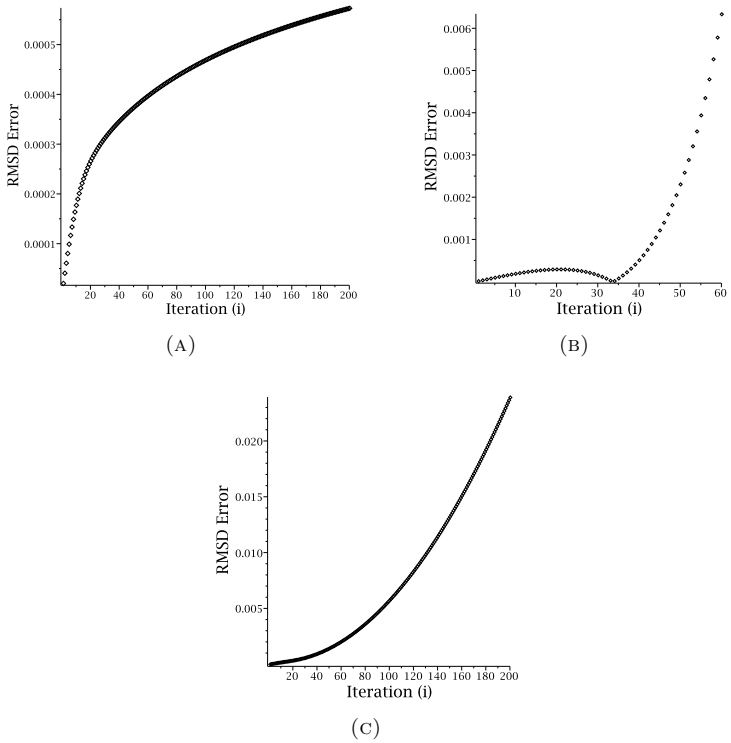

FIGURE 1. Nonholonomic Particle: rmsd errors for the (a) RDLA, (b) HDEL, and (c) PTHDEL algorithms.

The difference of two orders of magnitude in the rmsd errors between the PTHDEL and RDLA algorithms is explained by looking at how well they preserve the discrete energy. Figure 2 (parts (a)-(c)) below shows a comparison of the deviation of the discrete energies from one for each algorithm. While the RDLA and HDEL algorithms both have stable errors of order 10^{-4} (Figure 2 (a) and (b), respectively), Figure 2(c) shows that the PTHDEL algorithm's discrete energy values seem to grow linearly away from one. This is expected since, although the PTHDEL algorithm results in good long-term behavior for $E_{\tilde{\mathcal{L}}_c}$ (Figure 2(d)), since (50) here reads (recall $F(r) = (f(r))^{-1}$)

$$E_{l_c}(t) = 1 + \sqrt{1+x^2}E_{\tilde{\mathcal{L}}_c},$$

as $x(t)$ increases, since $E_{\tilde{\mathcal{L}}_c}$ remains roughly constant at $C \approx 5.2 \times 10^{-4}$, the t-time energy $E_{l_c}(t) - 1 \approx C\sqrt{x^2(t)} = Ct$, using (53). Such an increase in the energy contributes to the rmsd error over the long-term as well (Figure 1(c)).

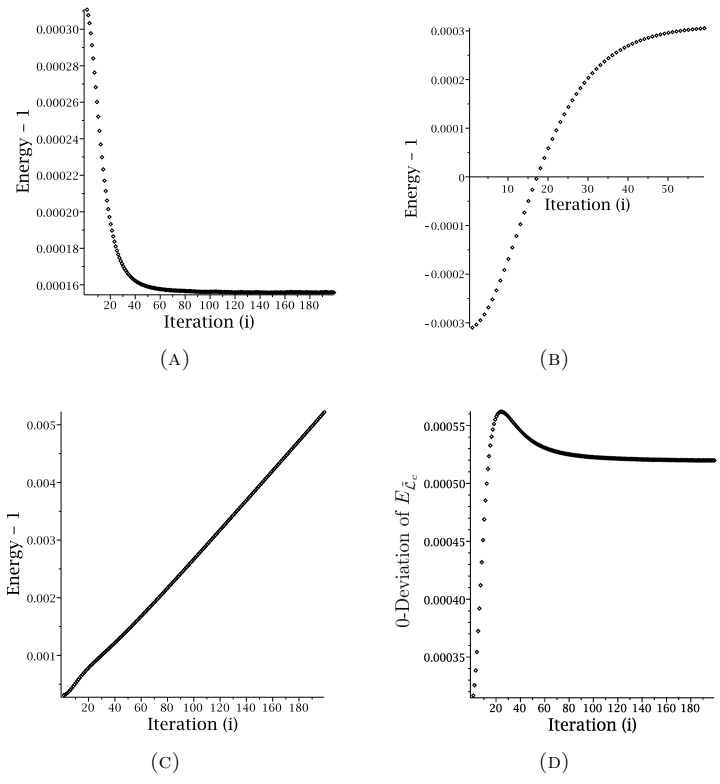

FIGURE 2. Nonholonomic Particle: deviation from one of the discrete energies for the (a) RDLA, (b) HDEL, and (c) PTHDEL algorithms, and (d) deviation from zero of the discrete energy $E_{\tilde{\mathcal{L}}_c}$ for the PTHDEL algorithm.

Figure 3 shows a comparison of the deviation from zero of each algorithm's discrete constraint values[7]. The constraint preservation error is smallest for the HDEL algorithm, of order 10^{-9}, followed by the RDLA and PTHDEL algorithms (both of order 10^{-8}).

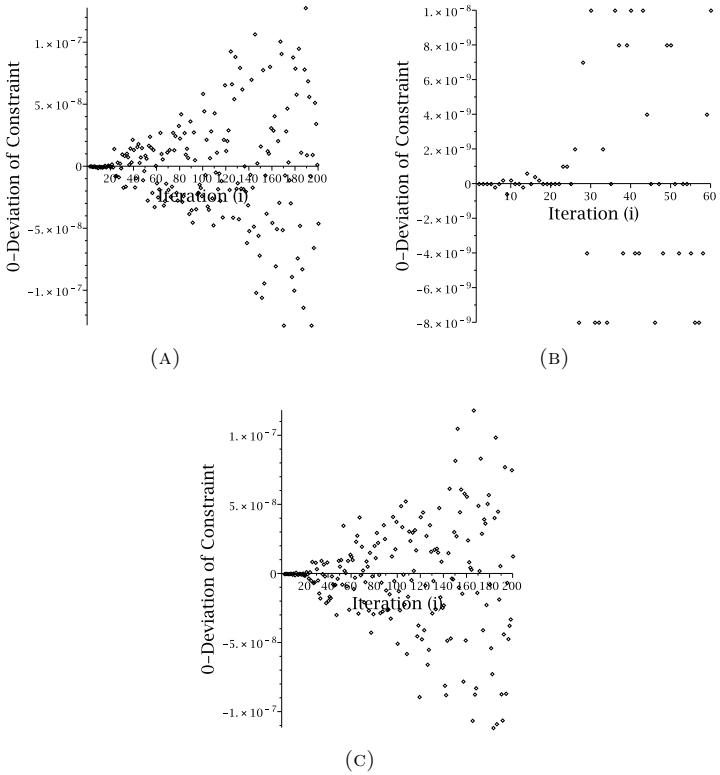

FIGURE 3. Nonholonomic Particle: constraint errors for the (a) RDLA, (b) HDEL, and (c) PTHDEL algorithms.

Lastly, let us illustrate the application of Proposition 1. From (56), it follows that $F''(x(\tau)) = \cosh(\tau)$. However, as discussed in Remark 1, one would not know this before running the HDEL algorithm. Therefore, let us discuss how one can find the bounds C_i of Proposition 1 using only the numerical results from the HDEL algorithm.

First, we note that from the x Euler-Lagrange equation of $\mathcal{L}_c$, it follows that

$$x'' = \frac{xx'^2}{1+x^2}. \tag{58}$$

Then, after finding $F''(x(\tau))$ using the chain rule, we can substitute in (58) to arrive at

$$F''(x(\tau)) = \frac{(x'(\tau))^2}{\sqrt{1+(x(\tau))^2}}. \tag{59}$$

[7]We have constructed this for each of the three integrators by plotting the discretization of the constraint $\dot{z} + x\dot{y}$, using the exact solution for z and the algorithm solution for x, y.

Since the HDEL algorithm shows that the discrete trajectory x_i is increasing for all τ (in agreement with (56)), then it follows that for all $\tau \in [\tau_{i-1}, \tau_i]$,

$$|F''(x(\tau))| \leq \frac{(x'(\tau))^2}{\sqrt{1+(x_{i-1})^2}} \lesssim \tilde{C}_i := \frac{(x_i - x_{i-1})^2}{(h_\tau)^2\sqrt{1+(x_{i-1})^2}}, \tag{60}$$

where, although we cannot precisely bound $x'(\tau)$, we have estimated it using the forward finite difference of the HDEL algorithm's discrete trajectories x_i. Using these bounds in Proposition 1, the errors $|\delta t_i|$ are computed to be

$$|\delta t_1| \approx 1.04 \times 10^{-5}, \quad |\delta t_2| \approx 2.09 \times 10^{-5}, \quad \dots \quad , |\delta t_{N_\tau}| \approx 2.14 \times 10^{-3}. \tag{61}$$

Since we *do* have the exact expression for $F''(x(\tau))$ after all, we can compare the approximate errors in (61) to the actual error bounds computed by using $|F''(x(\tau))| \leq C_i := |\cosh(\tau_i)|$ for $\tau \in [\tau_{i-1}, \tau_i]$. The rmsd difference between the error bounds C_i and $\tilde{C}_i$ for $|\delta t_i|$ is shown in Figure 4 below.

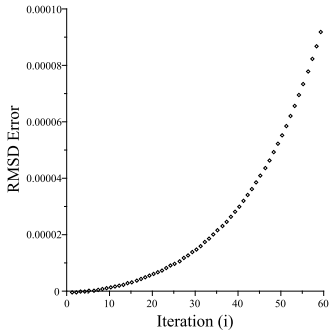

(A)

FIGURE 4. Nonholonomic Particle: rmsd difference between approximate and actual error bounds for $|\delta t_i|$ for the HDEL algorithm.

Figure 4, along with (61), shows that by using only the numerical results of the HDEL algorithm to approximate the unreparameterized values $r^\alpha(t(\tau_i))$ with the discrete values r_i^α produced from the HDEL algorithm, we incur an additional error in t of order at most 10^{-3}. Finally, we note that an alternative method to estimate the errors $|\delta t_i|$ is to compare the numerical results for two different orders of accuracy. This approach is at the heart of the Runge-Kutta-Fehlberg method [5].

5.2. **The sinusoidal nonholonomic particle.** To further illustrate the effect of the multiplier f on E_{l_c} described by (50), let us consider again the nonholonomic particle example, but instead with the constraint

$$\dot{z} = -(\sin x)\dot{y}.$$

This abelian Chaplygin nonholonomic system is again integrable by quadrature, and also Hamiltonizable with multiplier $f(x) = (1+\sin^2(x))^{-1/2}$. The solutions to the constrained nonholonomic equations (5), with $x_0 = 0$ and $\alpha_x, \alpha_y \neq 0$, are

$$x(t) = \alpha_x t, \quad y(t) = \frac{\alpha_y \mathbb{F}(\alpha_x t \,|\, -1)}{\alpha_x}, \tag{62}$$

where $\mathbb{F}(t|m)$ is the elliptic integral of the first kind [30] (Section 19). After Hamiltonization, the solutions (62) become

$$x(\tau) = \frac{1}{\alpha_x} am\left(\frac{\alpha_x \tau}{\alpha_y}, -1\right), \quad y(\tau) = \alpha_y \tau \tag{63}$$

in τ-time, where $am(\tau, m)$ is the Jacobi amplitude function [30] (Section 22.16).

Because $|F(x)| = \left|\sqrt{1+\sin^2(x)}\right| \leq 2$, we expect that the PTHDEL algorithm will have better long-term energy tracking than in the previous example, since by (50) this would lead to energy errors E_{l_c} of roughly the same order as that of $E_{\tilde{\mathcal{L}}_c}$. Using the same initial conditions as in the previous example, and again with $\epsilon = 0.5$, $N = N_\tau = 200$, $h = h_\tau = 0.5$, and the initial energy $E = 1$, Figure 5(c) below confirms this[8]. As the figure shows, for the sinusoidal nonholonomic particle system all three integrators have comparable long-term energy behavior, with errors of order 10^{-4}.

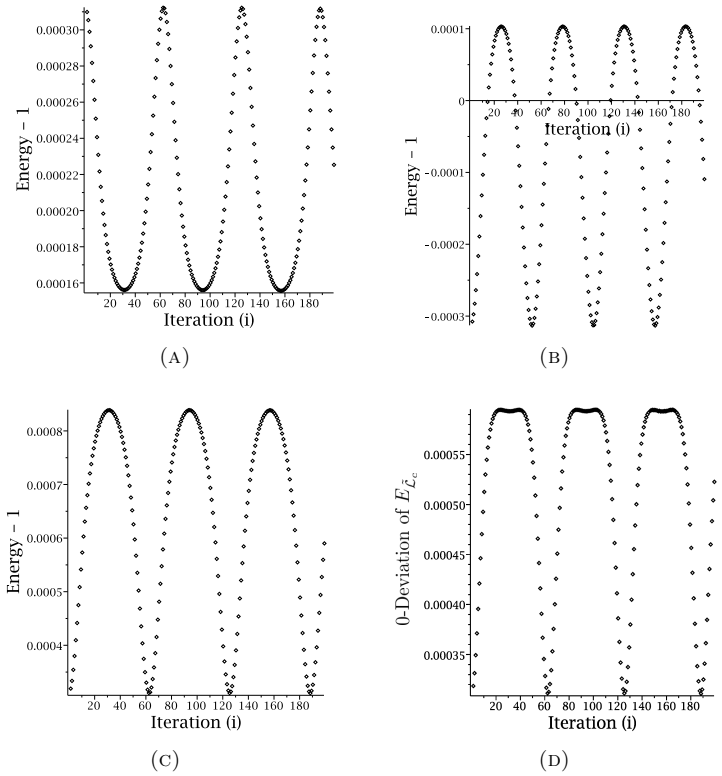

FIGURE 5. Sinusoidal Nonholonomic Particle: deviation from one of the discrete energies for the (a) RDLA, (b) HDEL, and (c) PTHDEL algorithms, and (d) deviation from zero of the discrete energy $E_{\tilde{\mathcal{L}}_c}$ for the PTHDEL algorithm.

[8] In fact, from (50) we can estimate the maximum error in E_{l_c}. Using the fact that the maximum error in $E_{\tilde{\mathcal{L}}_c}$ is 0.0006 (Figure 5(d)), along with $|F| \leq \sqrt{2}$, we estimate that $E_{l_c} - 1 \leq (0.0006)\sqrt{2} \approx 0.00085$, in agreement with the maximum error in Figure 5(c).

The corresponding rmsd errors are shown in Figure 6 below. The improved energy behavior of the PTHDEL algorithm has led to errors of the same order of magnitude as the RDLA algorithm by the end of the computation time (compare Figure 6, parts (a) and (c)). Figure 6(b) shows that the HDEL algorithm has the best long-term rmsd error behavior of the three algorithms.

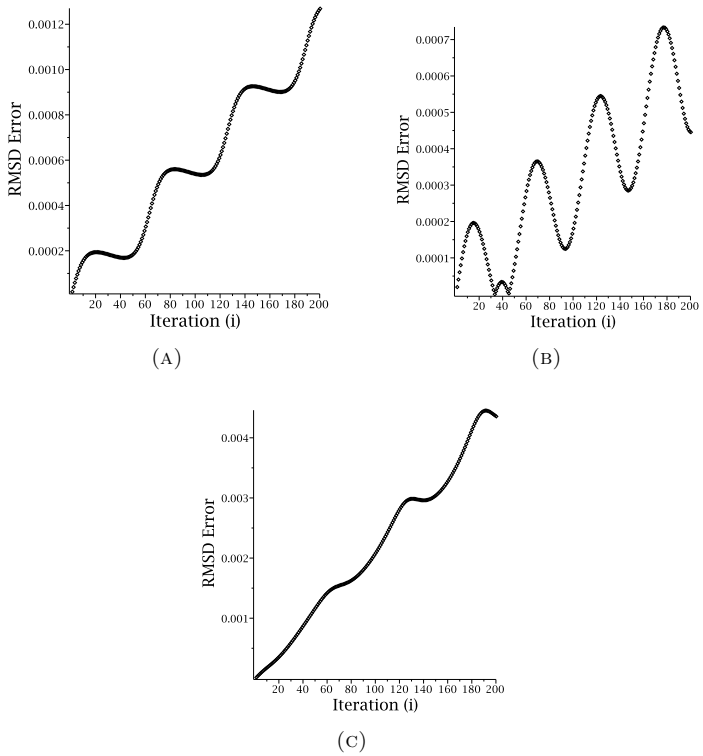

FIGURE 6. Sinusoidal Nonholonomic Particle: rmsd error for the (a) RDLA, (b) HDEL, and (c) PTHDEL algorithms.

Finally, Figure 7 below shows a comparison of the deviation from zero of each algorithm's discrete constraint values. Once again the HDEL algorithm produces the smallest errors (of order 10^{-9}) of the three algorithms (Figure 7(b)). The RDLA and PTHDEL algorithms both have comparable errors of order 10^{-8} (Figure 7, parts (a) and (c), respectively).

5.3. **The knife edge on an inclined plane.** Consider a plane slanted at an angle α from the horizontal and let (x, y) denote the position of the point of contact of a knife edge on the plane with respect to a fixed Cartesian coordinate system on the plane, see [1] (Section 1.6). Moreover, let φ represent the orientation of the knife edge with respect to the xy-axis. The Lagrangian and constraints are then given by

$$L = \frac{1}{2}\left(\dot{x}^2 + \dot{y}^2 + \dot{\varphi}^2\right) + x \sin\alpha, \qquad \dot{y} - \dot{x}\,\tan\varphi = 0, \tag{64}$$

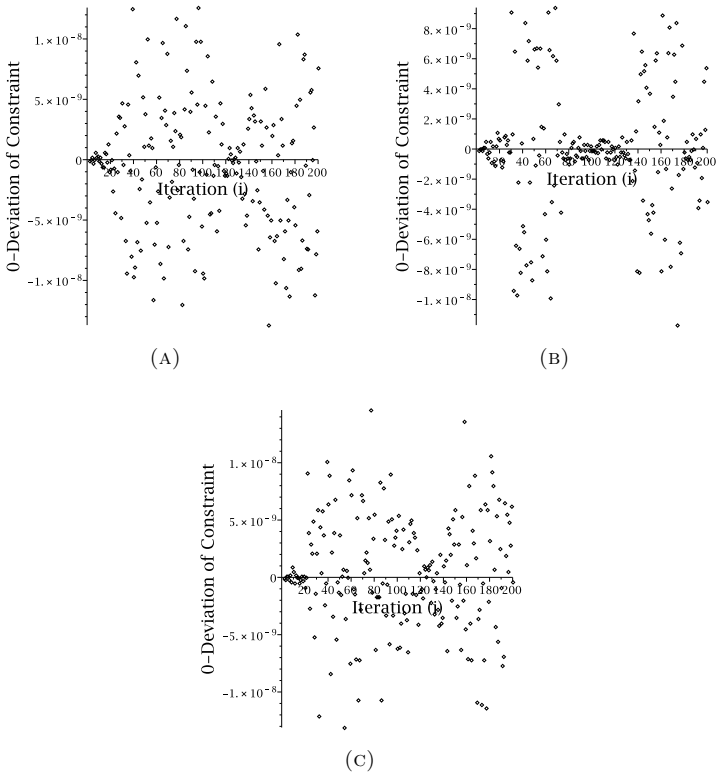

FIGURE 7. Sinusoidal Nonholonomic Particle: constraint errors for the (a) RDLA, (b) HDEL, and (c) PTHDEL algorithms.

where we have set all parameters (mass, moment of inertia, and the gravitational acceleration) equal to one for simplicity. The system is again Chaplygin Hamiltonizable with $f(\varphi) = \cos\varphi$, [13]. Now, although f has zeros, this will not prevent the application of the results obtained thus far. Indeed, we have that

$$\mathcal{L}_c = \frac{1}{2}(x'^2 + \cos^2\varphi\,\varphi'^2) + x\sin\alpha.$$

The reduced equations of motion are once again integrable by quadrature [13], and taking $\varphi(0) = x(0) = 0$ and $\omega := \dot{\varphi}(0) \neq 0$ yields the nonholonomic solutions

$$x(t) = \frac{\sin\alpha}{2\omega^2}\sin^2(\varphi(t)) + \frac{\kappa}{\omega}\sin\varphi(t), \qquad \varphi(t) = \omega t, \tag{65}$$

where $\kappa := \dot{x}(0)$. The time reparameterization $d\tau = f(\varphi)\,dt = \cos(\varphi(t))\,dt$ can once again be integrated explicitly to obtain

$$\tau(t) = \frac{1}{\omega}\sin(\varphi(t)), \tag{66}$$

where we have again set $\tau(t=0) = 0$ for simplicity. We can invert this to obtain the τ-time version of the solutions (65):

$$x(\tau) = \frac{\sin\alpha}{2}\tau^2 + \kappa\tau, \quad \varphi(\tau) = \arcsin(\omega\tau), \tag{67}$$

where we choose the branch of the inverse sine function based on the values of $\varphi(t)$. Moreover, since (66) shows that $|\tau(t)| \leq \frac{1}{\omega}$, we conclude that although the solutions (67) are only defined for $\tau \in [-\frac{1}{\omega}, \frac{1}{\omega}]$, the change in branch cut for the inverse sine function as φ crosses $\frac{\pi}{2}$ implies that (67) represents periodic motion, in agreement with the t-time solutions (65).

For our numerical simulations of the knife edge on the inclined plane, we chose the initial conditions $x(0) = \varphi(0) = 0$ and $\kappa = \omega = 1$, and set the incline angle $\alpha = 5°$. We again selected to symmetrize the Lagrangians used, with $\epsilon = 0.5$, and chose $N = 100$, $h = h_\tau = 0.07$. Thus, our total simulation time in t-time is $hN = 7$ seconds.

Now, since $f(\varphi)$ has roots this means that the corresponding simulation time in τ-time is $\tau(hN) = \tau(7)$, which is approximately 0.66 seconds, computed from (66). Thus, we have chosen $N_\tau = N = 100$ for the number of iterations in τ-time.

The comparison of the rmsd errors is shown in Figure 8 below. The RDLA algorithm leads to the smallest rmsd error (of order 10^{-3}), followed by the HDEL algorithm (of order 10^{-3}) and finally the PTHDEL algorithm (of order 10^{-2}). The abrupt behavior encountered by all the algorithms near iteration numbers $i = 23$ and $i = 68$ is a result of the fact that $\varphi(23h) \approx \frac{\pi}{2}$ and $\varphi(68h) \approx \frac{3\pi}{2}$. Near these values l_c, which depends on $\sec\varphi$, becomes singular. Similarly, since the Lagrangians $\mathcal{L}_c$ and $\tilde{\mathcal{L}}_c$ for the knife edge are

$$\begin{aligned} \mathcal{L}_c &= \frac{1}{2}\left(x'^2 + (\cos^2\varphi)\varphi'^2\right) + x\sin\alpha \\ \tilde{\mathcal{L}}_c &= \frac{1}{2}\left((\sec\varphi)\dot{x}^2 + (\cos\varphi)\dot{\varphi}^2\right) + \cos\varphi(x\sin\alpha + 1), \end{aligned} \tag{68}$$

near those two iteration points the numerical solver is again attempting to continue the algorithm despite approaching a singularity (as is the case for $\mathcal{L}_c$, Figure 8(c)), or approaching a vertical tangent at $\arcsin(\pm 1)$ (as is the case for $\tilde{\mathcal{L}}_c$, Figure 8(b)).

Figure 9 below shows a comparison of the discrete energy errors for the three algorithms. The PTHDEL algorithm has the best long-term performance, with errors of order 10^{-2} (although these errors increase as the algorithm approaches the aforementioned iteration values $i = 23$ and $i = 68$). The RDLA and HDEL algorithms both have errors of order 10^{-1}. Figure 10 below compares how well the three algorithms numerically preserve the nonholonomic constraint. All three algorithms lead to errors of order 10^{-9}.

6. Conclusion.

We have developed two new numerical algorithms to simulate the mechanics of Chaplygin Hamiltonizable nonholonomic systems, the HDEL and PTHDEL algorithms defined by (33) and (46), respectively. The development of these two new integrators was based on the assumption that the underlying nonholonomic system was Chaplygin Hamiltonizable. Although it is certainly not true that every nonholonomic system is Chaplygin Hamiltonizable, in [2] necessary and sufficient conditions were derived in the form of a coupled set of linear first-order partial differential equations for f whose solution, if there is one, determines the multiplier, up to a constant. Practically speaking then, given a nonholonomic system one can check its Chaplygin Hamiltonizability (using a symbolic software package, like MAPLE), find f, and then apply one of the two integrators developed

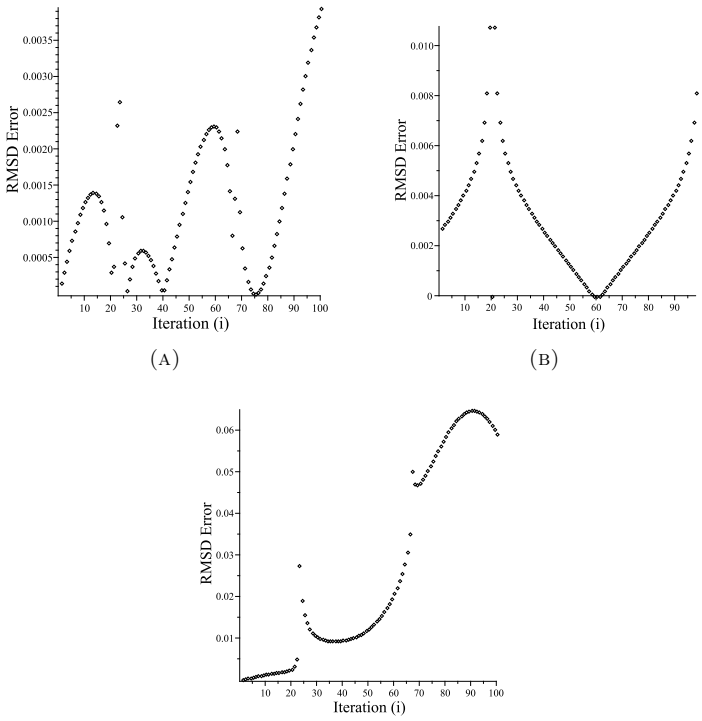

FIGURE 8. Knife Edge on Inclined Plane: rmsd error for the (a) RDLA, (b) HDEL, and (c) PTHDEL algorithms.

herein. By then exploiting the Hamiltonian form of the time reparameterized reduced nonholonomic equations, these new algorithms allow the application of variational integrators to non-Hamiltonian nonholonomic systems which are Chaplygin Hamiltonizable.

The HDEL algorithm (33) proceeds in the reparameterized time τ, and our numerical examples above indicate that it generally leads to superior long-term discrete constraint preservation behavior relative to the RDLA nonholonomic integrator. The examples also suggest that the long-term discrete energy behavior compares well with the RDLA algorithm. Moreover, the fact that the HDEL algorithm proceeds in τ-time does not affect its usefulness. As the Example 5.1 showed, for small enough timesteps h these errors δt_i can be very small. As an alternative, instead of insisting on a smaller timestep to improve this error one can always apply a higher-order quadrature rule to (34) to reduce the error in assigning a discrete t value to each discrete τ value used in the algorithm.

However, in case one is interested in attempting to preserve the equal timesteps in t-time, a possibility for future research would be to add the holonomic constraints $h = \int_{\tau_i}^{\tau_{i+1}} F(r(\tilde{\tau}))\, d\tilde{\tau}$, $i = 1, \ldots, N_\tau - 1$, to the unconstrained Hamiltonian system defined by the Hamiltonized Lagrangian $\mathcal{L}_c$. By defining the box functions $\chi_{i,i+1}(\tau)$ to be equal to unity for $\tau \in [i, i+1] \subset [0, N]$ and zero otherwise, one could express

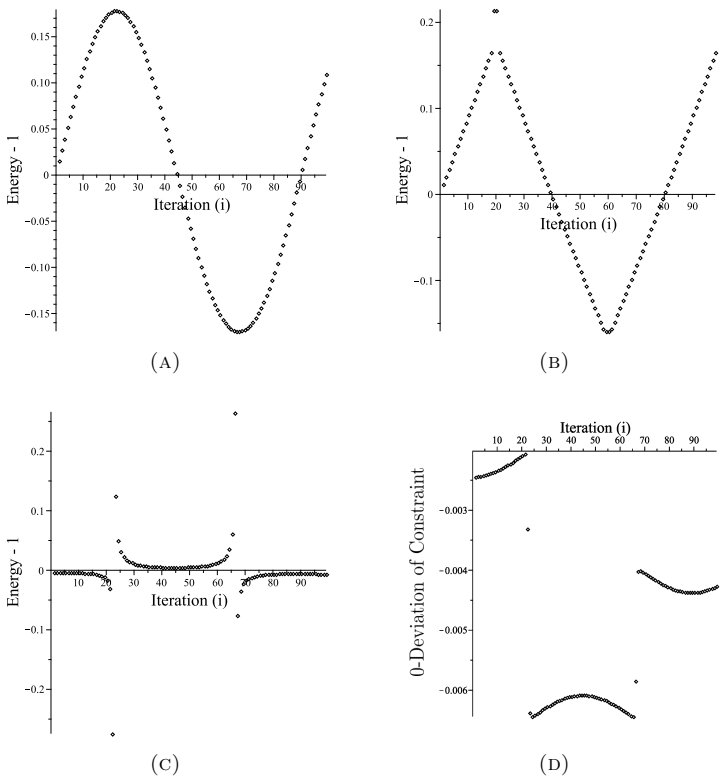

FIGURE 9. Knife Edge on Inclined Plane: deviation from one of the discrete energies for the (a) RDLA, (b) HDEL, and (c) PTHDEL algorithms, and (d) deviation from zero of the discrete energy $E_{\tilde{\mathcal{L}}_c}$ for the PTHDEL algorithm.

these constraints as $h = \int_0^{N_\tau} \chi_{i,i+1}(\tilde{\tau}) F(r(\tilde{\tau}))\, d\tilde{\tau}$, $i = 1, \ldots, N_\tau - 1$. These constraints then take the form of isoperimetric constraints (see Section 4.3.2 of [33]). One could then apply a holonomic variational integrator, [27], to the new system, and expect the resulting integrator to have roughly fixed timesteps h without the need (but also without the freedom) of selecting a quadrature rule for (34).

The PTHDEL algorithm, a new application of the Poincaré transformation to nonholonomic mechanics, also seems to compare well with the RDLA nonholonomic integrator for multipliers f which are either bounded or show long-term growth. For this class of multipliers, the PTHDEL algorithm inherits the favorable long-term discrete energy behavior from the variational integrator it is based on. Moreover, as the knife edge example shows, the PTHDEL algorithm may even have superior long-term behavior relative to the RDLA integrator for multipliers with roots.

Let us conclude by indicating two more intriguing directions for future research. We note first that despite the requirement that the nonholonomic system under consideration be Chaplygin Hamiltonizable in order to apply the new integrators developed here, different techniques exist for the Hamiltonization of nonholonomic systems [12]. In particular, in [2], Hamiltonization is accomplished by directly

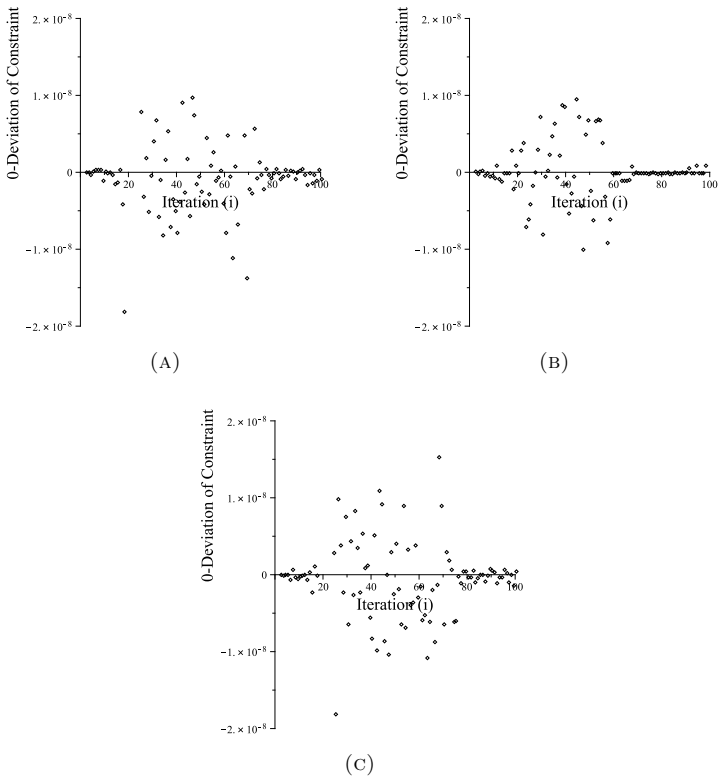

FIGURE 10. Knife Edge on Inclined Plane: constraint errors for the (a) RDLA, (b) HDEL, and (c) PTHDEL algorithms.

solving the inverse problem of the calculus of variations. This method of Hamiltonization is then used in [29] to simulate the dynamics of a class of nonholonomic systems using variational integrators. It is within the realm of possibility that one could combine the results of [2] with the results of [15,] on Chaplygin Hamiltonizability to enlarge the class of Hamiltonizable nonholonomic systems. The idea would be to solve the inverse problem of the calculus of variations for a suitably reparameterized reduced nonholonomic system, where the reparameterization function f need not be what we have hitherto called the multiplier. As in [2], one would expect a family of Lagrangians as solutions. This freedom to choose the Lagrangian could be used to develop more accurate and efficient numerical methods for these Hamiltonized systems. In addition, for nonholonomic systems on Lie groups, an analogous process to Hamiltonization called Poissonization, discussed in [15], could be used to develop variational integrators applicable to Poissonizable nonholonomic systems. A comparison of these results with the works of [11, 20, 28] would be interesting.

Finally, we wish to mention that although we have restricted ourselves here in basing the development of our two new integrators on the simplest quadrature rule for the Lagrangian (13), one could certainly use more advanced quadrature rules as

a starting point. In particular, the quadrature rules used in the Galerkin Hamiltonian Variational Integrators and Symplectic Partitioned Runge-Kutta methods, discussed recently in [25], appear to be promising and worth pursuing.

Acknowledgments. The research of OEF was supported by the Institute for Mathematics and its Applications through its Postdoctoral Fellowship Program. AMB was supported through NSF grants DMS-0907949, DMS-0806756 and DMS-1207693. PJO was supported through NSF grant DMS-0807317. OEF would also like to thank Alexander Alekseenko and Tom Mestdag for helpful discussions throughout the preparation of the paper.

REFERENCES

[1] A. M. Bloch, "Nonholonomic Mechanics and Control," Interdisciplinary Applied Mathematics, **24**, Systems and Control, Springer-Verlag, New York, 2003.
[2] A. M. Bloch, O. E. Fernandez and T. Mestdag, *Hamiltonization of nonholonomic systems and the inverse problem of the calculus of variations*, Rep. Math. Phys., **63** (2009), 225–249.
[3] A. V. Borisov and I. S. Mamaev, *Rolling of a rigid body on plane and sphere. Hierarchy of dynamics*, Reg. Chaotic Dyn., **7** (2002), 177–200.
[4] A. V. Borisov and I. S. Mamaev, *Conservation laws, hierarchy of dynamics and explicit integration of nonholonomic systems*, Reg. Chaotic Dyn., **13** (2008), 443–490.
[5] R. L. Burden and J. D. Faires, "Numerical Analysis," 8^{th} edition, Thomson Brooks/Cole, Belmont, CA, 2005.
[6] S. A. Chaplygin, *On a ball's rolling on a horizontal plane*, (in Russian), Mat. Sbornik, **24** (1903), 139–168; (in English), Reg. Chaotic Dyn., **7** (2002), 131–148.
[7] S. A. Chaplygin, *On the theory of motion of nonholonomic systems. The reducing-multiplier theorem*, (in Russian), Mat. Sbornik, **28** (1911), 303–314; (in English), Reg. Chaotic Dyn., **13** (2008), 369–376.
[8] J. Cortés Monforte, "Geometric, Control and Numerical Aspects of Nonholonomic Systems," Lecture Notes in Mathematics, **1793**, Springer-Verlag, Berlin, 2002.
[9] J. Cortés Monforte and S. Martínez, *Nonholonomic integrators*, Nonlinearity, **14** (2001), 1365–1392.
[10] Y. N. Fedorov and B. Jovanović, *Quasi-Chaplygin systems and nonholonomic rigid body dynamics*, Lett. Math. Phys., **76** (2006), 215–230.
[11] Y. N. Fedorov and D. V. Zenkov, *Discrete nonholonomic LL systems on Lie Groups*, Nonlinearity, **18** (2005), 2211–2241.
[12] O. E. Fernandez, "The Hamiltonization of Nonholonomic Systems and its Applications," Ph.D. Thesis, The University of Michigan, 2009.
[13] O. E. Fernandez and A. M. Bloch, *The Weitzenböck connection and time reparameterization in nonholonomic mechanics*, J. Math. Phys., **52** (2011), 012901, 18 pp.
[14] O. E. Fernandez and A. M. Bloch, *Equivalence of the dynamics of nonholonomic and variational nonholonomic systems for certain initial data*, J. Phys. A, **41** (2008), 344005, 20 pp.
[15] O. E. Fernandez, T. Mestdag and A. M. Bloch, *A generalization of Chaplygin's reducibility theorem*, Reg. Chaotic Dyn., **14** (2009), 635–655.
[16] P. Fitzpatrick, "Advanced Calculus," 2^{nd} edition, Thomson Brooks/Cole, Belmont, CA, 2006.
[17] M. R. Flannery, *The enigma of nonholonomic constraints*, Am. J. of Phys., **73** (2005), 265–272.
[18] Z. Ge and J. E. Marsden, *Lie-Poisson Hamilton-Jacobi theory and Lie-Poisson integrators*, Phys. Lett. A, **133** (1988), 134–139.
[19] E. Hairer, *Variable time step integration with symplectic methods*, Appl. Numer. Math., **25** (1997), 219–227.
[20] D. Iglesias, J. C. Marrero, D. M. de Diego and E. Martínez, *Discrete nonholonomic Lagrangian systems on Lie groupoids*, J. Nonlinear Sci., **18** (2008), 221–276.
[21] M. Kobilarov, J. E. Marsden and G. S. Sukhatme, *Geometric discretization of nonholonomic systems with symmetries*, Discrete and Continuous Dynamical Systems, Series S, **3** (2010), 61–84.

[22] D. Korteweg, Ü*ber eine ziemlich verbreitete unrichtige Behandlungsweise eines Problemes der rollenden Bewegung und insbesondere* über *kleine rollende Schwingungen um eine Gleichgewichtslage*, Nieuw Archiefvoor Wiskunde, **4** (1899), 130–155.
[23] B. Leimkuhler and S. Reich, "Simulating Hamiltonian Dynamics," Cambridge Monographs on Applied and Computational Mathematics, **14**, Cambridge Univ. Press, Cambridge, 2004.
[24] B. Leimkuhler and R. Skeel, *Symplectic numerical integrators in constrained Hamiltonian systems*, J. Computational Phys., **112** (1994), 117–125.
[25] M. Leok and J. Zhang, *Discrete Hamiltonian variational integrators*, IMA J. Numerical Analysis, **31** (2011), 1497–1532.
[26] J. E. Marsden and T. S. Ratiu, "Introduction to Mechanics and Symmetry. A Basic Exposition of Classical Mechanical Systems," 2^{nd} edition, Texts in Applied Mathematics, **17**, Springer-Verlag, New York, 1999.
[27] J. E. Marsden and M. West, *Discrete mechanics and variational integrators*, Acta Numerica, **10** (2001), 357–514.
[28] R. McLachlan and M. Perlmutter, *Integrators for nonholonomic mechanical systems*, J. Nonlinear Sci., **16** (2006), 283–328.
[29] T. Mestdag, A. M. Bloch and O. E. Fernandez, *Hamiltonization and geometric integration of nonholonomic mechanical systems*, in "Proc. 8 th Nat. Congress on Theor. and Applied Mechanics," Brussels, Belgium, (2009), 230–236, arXiv:1105.5223.
[30] F. W. J. Olver, D. W. Lozier, R. F. Boisvert and C. W. Clark, eds., "NIST Handbook of Mathematical Functions," U.S. Department of Commerce, National Institute of Standards and Technology, Washington, DC; Cambridge Univ. Press, Cambridge, MA, 2010.
[31] T. Ohsawa, O. E. Fernandez, A. M. Bloch and D. V. Zenkov, *Nonholonomic Hamilton-Jacobi theory via Chaplygin Hamiltonization*, J. Geometry and Phys., **61** (2011), 1263–1291.
[32] J. Ryckaert, G. Ciccotti and H. Berendsen, *Numerical integration of the cartesian equations of motion of a system with constraints: Molecular dynamics of n-alkanes*, J. Computational Phs., **23** (1977), 327–341.
[33] B. van Brunt, "The Calculus of Variations," Universitext, Springer-Verlag, New York, 2004.
[34] L. Verlet, *Computer experiments on classical fluids*, Phys. Rev., **159** (1967), 98–103.

Received May 2011; revised October 2011.

E-mail address: ofernand@wellesley.edu
E-mail address: abloch@umich.edu
E-mail address: olver@umn.edu